JOURNAL OF combinatorial CHEMISTRY

Volume 3, Number 1 January/February 2001

Reports

Determination of Functional Group Distribution within Rasta Resins Utilizing Optical Analysis

Shelli R. McAlpine,*,† Craig W. Lindsley,‡ John C. Hodges,* Daniele M. Leonard, and G. Fredrick Filzen

Department of Chemistry, Pfizer Global Research and Development, Ann Arbor Laboratories, 2800 Plymouth Road, Ann Arbor, Michigan 48105

Received July 28, 2000

In recent reports from the laboratories at Parke-Davis,[1] solid-supported living free radical polymerization (LFRP), initiated thermally by exposure of TEMPO-methyl resin **1** to styrenyl monomers **2**, was employed to access large, high loading isocyanate and silyl resins. These new resins (**3**) were coined "Rasta resins" and were believed to have a unique macromolecular architecture typified by long straight chain polymers bearing the desired functional groups that emanate from the phenyl groups of a cross-linked polystyrene core. In Scheme 1, the initially proposed architecture of a generic Rasta resin can be depicted by a cartoon structure (**4**) in which hair-like appendages represent new polymer growth from the original cross-linked bead. Alternatively, Rasta resins can be depicted by **5** wherein the shaded inner circle represents the original cross-linked core while the outer clear circle represents new polymer growth. Our attention now centered on elucidation of the functional group distribution within Rasta resins.

Recently, McAlpine and Schreiber disclosed an optical analysis protocol, previously used for analyzing biological

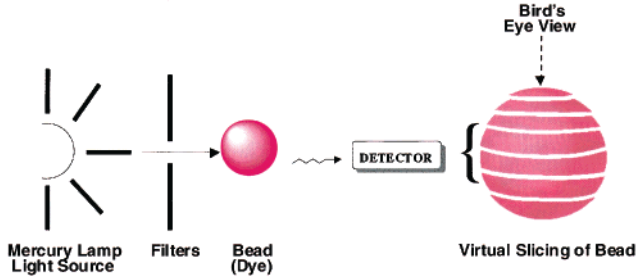

Figure 1. General concept of optical analysis.

Scheme 1. Rasta Resins

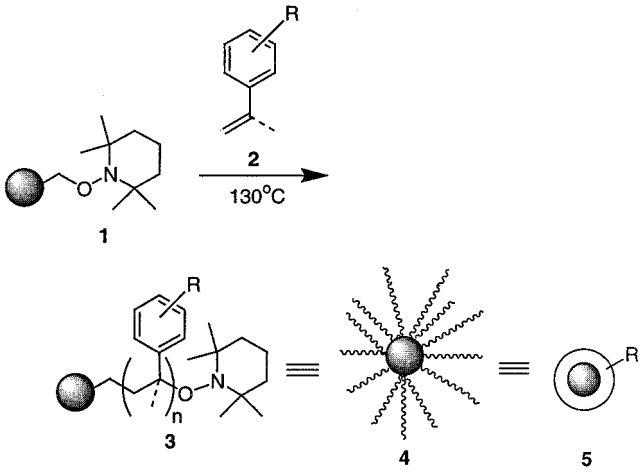

structures, to accurately visualize functional group distribution within a number of solid-support beads.[2] In this report, optical analysis is employed to analyze Rasta resins, and these data are then compared to data previously obtained for post-functionalized polystyrene (PS-*pf*), TentaGel, and ArgoPore resin beads as well as new data for poly(styrene-*co*-vinylbenzyl-chloride-*cross*-divinylbenzene), PS-*co* (*co*-polymerized polystyrene, Merrifield resin). The optical analysis technique employed herein allows for the visual cross sectioning (slicing) in 5−10 μm increments of fluorophore labeled beads (Figure 1), in which a rhodamine dye

* To whom correspondence should be addressed. J. Hodges: tel (734) 622-7731; fax (734) 622-3107; e-mail Jack.Hodges@pfizer.com S. McAlpine: tel (619) 594-5580; e-mail mcalpine@chemistry.sdsu.edu.

† Current address: Department of Chemistry and Biochemistry, San Diego State University, 5500 Campanile Dr., San Diego, CA 92182-1030.

‡ Current address: Lilly Research Laboratories, Eli Lilly & Company, Indianapolis, IN.

10.1021/cc000068a CCC: $20.00
Published on Web 12/14/2000

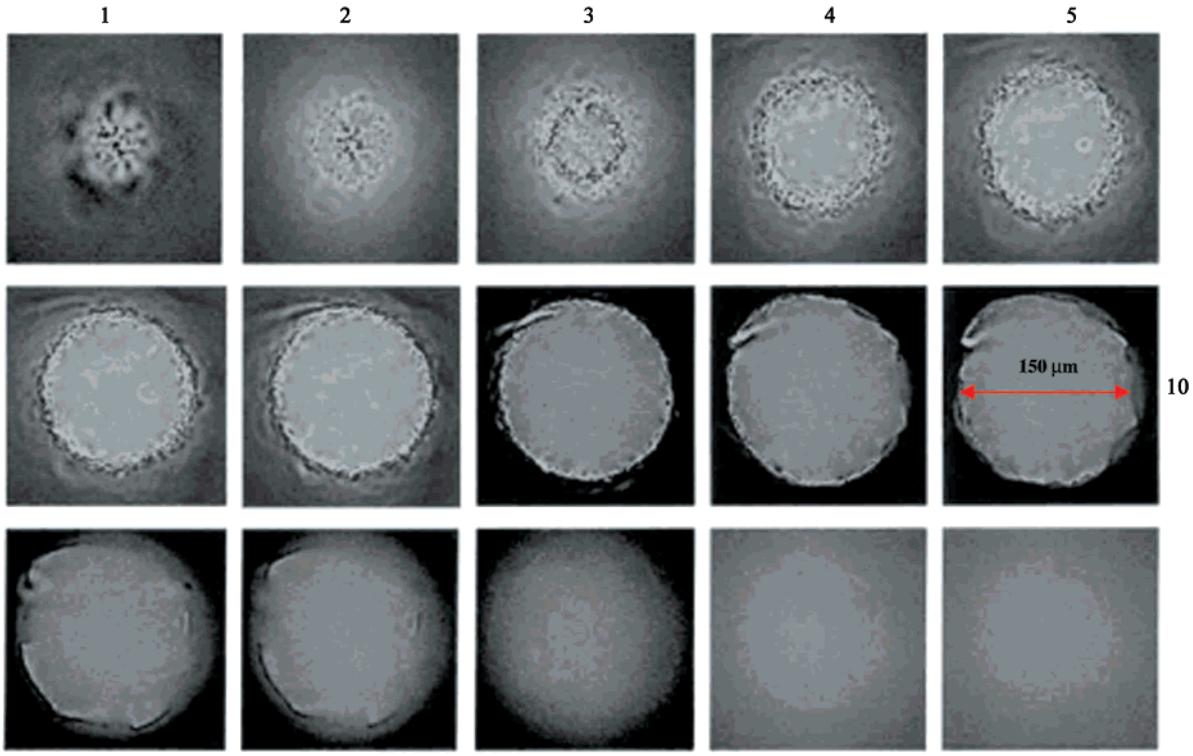

Figure 2. Optical slices of Rasta resin.

is covalently attached to the beads. By collection of the fluorescence emissions of the fluorophore on each bead cross section, the distribution of the dye moieties, and hence the pendant functional groups, can be accurately determined. More specifically, this protocol uses a mercury lamp to excite the covalently linked rhodamine fluorophore followed by detection of the wavelength-specific emission of the fluorophore allowing visualization of the dye distribution. The detector collects the fluorophore's emission from the bead directly from the point source as well as emission from the first-order diffraction pattern allowing for relatively opaque objects to be visually sliced as the focal plane is moved along the *z* axis. Then, a mathematical algorithm is employed to determine the original position of the light, providing a picture of the functional site distribution of dry, unswollen resin beads.

To visualize the location of functional sites by optical analysis, we attached a rhodamine dye to our isocyanate Rasta resin **6** [prepared from poly(styrene-*co*-vinylbenzylchloride-*cross*-divinylbenzene)] via a propylenediamine linker (Scheme 2) affording fluorescent resin **7**. At every step, couplings were performed in triplicate, where complete coupling was judged using a qualitative test (Kaiser-ninhydrin) and further confirmed by elemental analysis. Thus, each isocyanate moiety should be covalently linked to a rhodamine molecule allowing the site to be visualized by excitation of the dye at 540 nm and collection of emission light at 570 nm.

The aforementioned optical analysis technique was used to obtain the optical slices of the Rasta resin shown in Figure 2. The first 10 slices are images that are taken 5 μm apart until reaching the center of the bead (slice 10). These slices have no depth per se but are images that show the same

Scheme 2. Synthesis of Fluorescent Beads

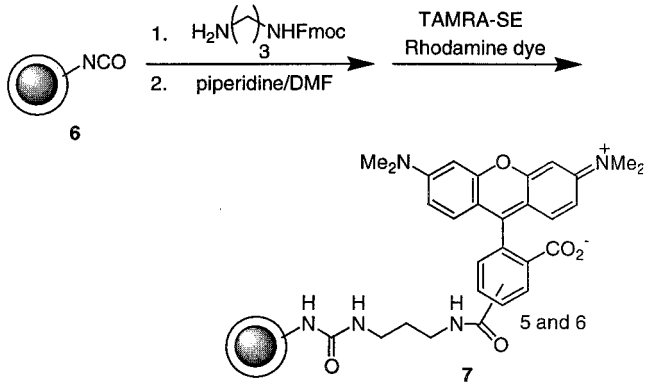

data one would see if one took the bead and cut it, for example, in half: the resulting image would be seen in slice 10. If one cut 20 μm from the top, one would see the image in slice 4. As one slices further away from the light source, the clarity of the image is reduced due to greater light diffusion. Thus only five slices are taken, 10 μM apart, through the bottom half of the bead. This phenomenon is most easily seen in the bottom two slices which are barely visible against the background due to some light being diffused in the above portion of the polymer bead. However, it is observed that regardless of orientation, each bead demonstrates results identical to those shown in Figure 2. The even distribution of dye seen in Figure 2 on each cross section implies that reagents diffuse completely throughout the resin bead core during both the LFRP functionalization and subsequent coupling process. Plotting the fluorescence intensity as a function of bead diameter for Rasta resin **7** illustrates a highly uniform distribution of functional sites throughout the resin bead (Figure 3).[3] Comparison of this result with those previously obtained for PS-*pf*, TentaGel,

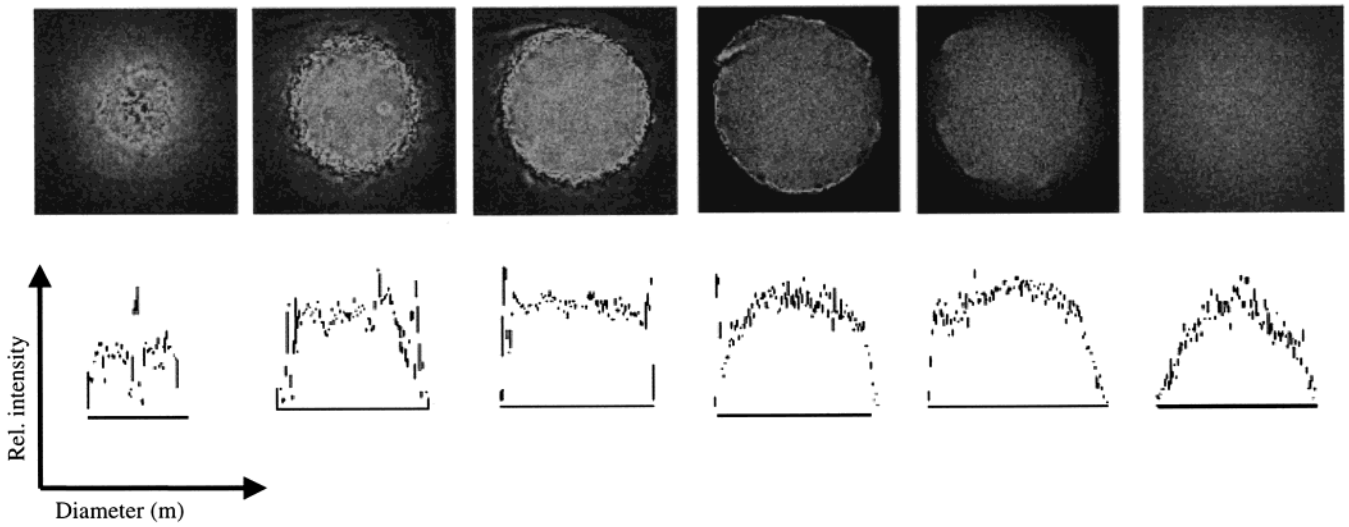

Figure 3. Fluorescence intensity across the diameter of Rasta resin.

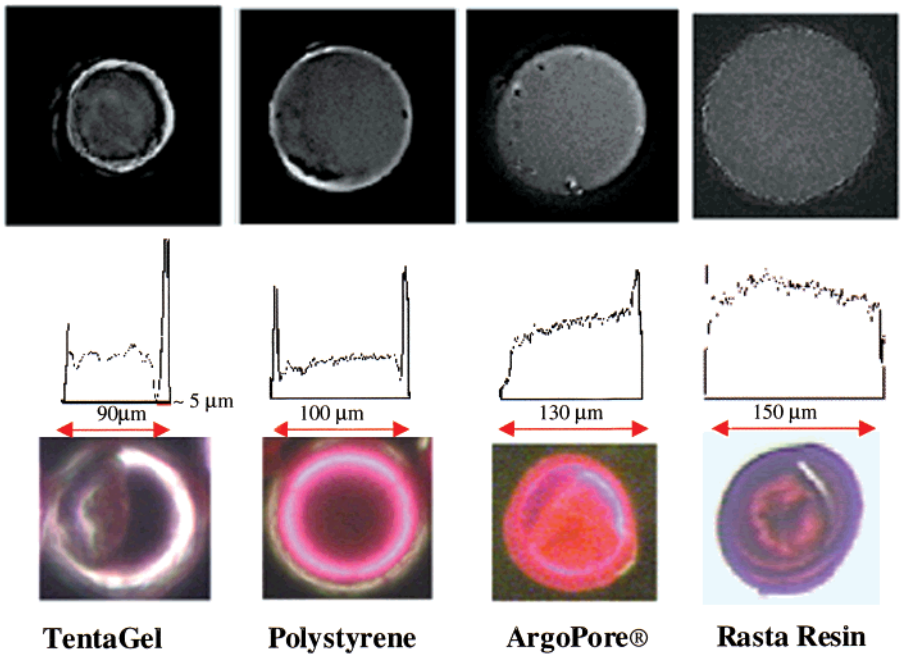

Figure 4. Comparison of all four resins.

and ArgoPore (Figure 4) clearly shows dramatic differences. The intensities of the Rasta resin and ArgoPore cross sections show uniform distribution throughout the bead diameter, with the Rasta beads displaying considerably less clustering than ArgoPore. The Rasta beads are fundamentally distinct from PS-*pf* and TentaGel as both of these two have a functionalized "shell" with clustering of dye seen on the bead's outer 5−10 μm. This shell for PS-*pf* and TentaGel comprises 30−35% and 40−60%, respectively, of the functional groups on each slice. In contrast it is estimated that about 10% of the dye resides on the outer 5 μm of each Rasta slice, establishing the uniform functionalization. These claims are further validated by examination of optical photographs (color photo inserts in Figure 4) of the four resins in the absence of fluorescence excitation which illustrate the same functional group distribution seen using optical analysis.

The TEMPO methyl resin **1** for the current study was prepared from poly(styrene-*co*-vinylbenzyl-chloride-*cross*-divinylbenzene), PS-*co* (*co*-polymerized polystyrene, Merrifield resin) and not the post-functionalized polystyrene, PS-*pf*, featured earlier. For comparison, a fluorescent PS-*co* based congener was prepared and examined by optical analysis. The fluorescent data obtained for PS-*co*, unlike that seen with PS-*pf*, which demonstrated a functionalized 5−10 μm shell surrounding the outer rim of the bead, displayed relative uniform functionalization across the diameter of the bead (Figure 5). Although the shaped images in Figure 5 are irregular, the beads look very spherical under a regular microscope, and the irregular distribution of the dye is responsible for the irregular image. The dye is distributed throughout the bead based on the sites created during the polymerization process. These sites are expected to vary to some extent and produce clustering in some areas based simply on the nature of any radical reaction. These data for PS-*co* were similar to that seen in several other studies done on polystyrene resins which have indicated a uniform distribution of functionality in polystyrene beads.[4] One study in particular was an autoradiograph experiment performed

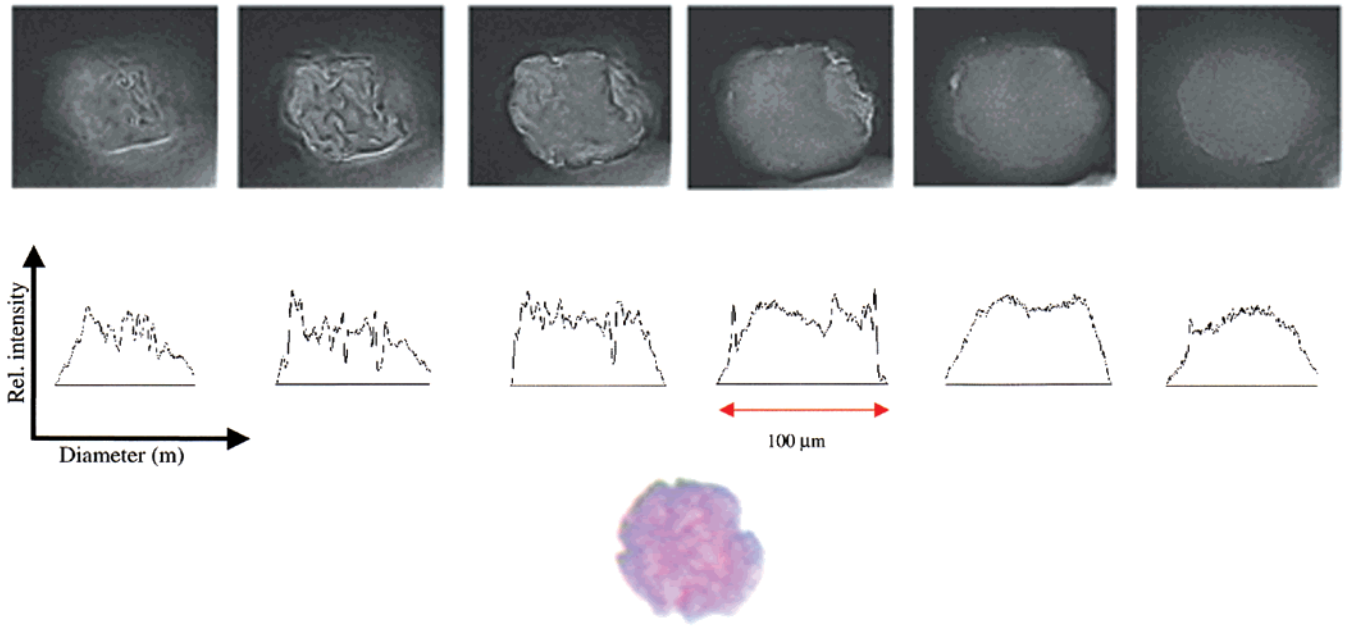

Figure 5. Fluorescence intensity across the diameter of copolymerized polystyrene.

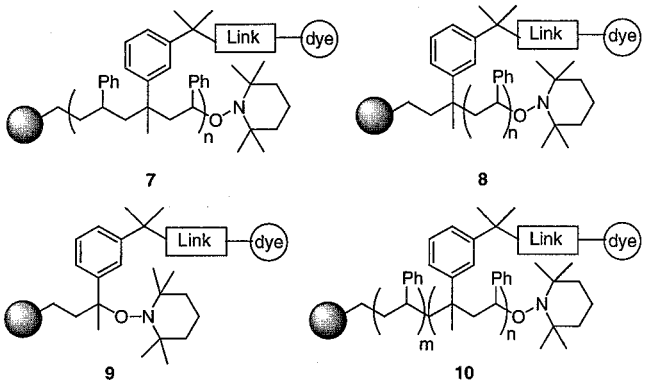

Figure 6. Architecture of Rasta resins for optical analysis.

by Merrifield[4a] suggesting the possibility that the autoradiograph may have been performed on PS-*co*.[5] Note that there is a relatively large discrepancy between the functional group distribution in PS-*pf* and PS-*co* (Figures 4 and 5). By comparison, Rasta resin **7** displays less clustering than the relatively evenly distributed PS-*co*.

Intrigued by these results, we prepared three other Rasta resins for study beginning with PS-*co* derived **1**. One of the prominent features of Rasta resins is the ability to control the macromolecular architecture of the bead.[1] By judicious selection of co-monomers in the LFRP step, the spacing of pendant functionalities from both the resin core and each other can be controlled. Rasta resins **8**, **9**, and **10** (Figure 6) feature macromolecular architecture different from that of **7** and were prepared according to our published procedures[1] and functionalized in accord with Scheme 1. Optical analysis data (Figure 7) show significant differences in functional group distribution among the three Rasta resins examined. Incorporation of a single 3-isopropenyl-α,α-dimethylbenzyl isocyanate (TMI) molecule at each TEMPO terminus followed by a second LFRP step with a 90 molar excess of styrene and subsequent functionalization provides resin **8**, a resin where the dye should be encased in a shell of unfunctionalized polystyrene. Optical analysis reveals a

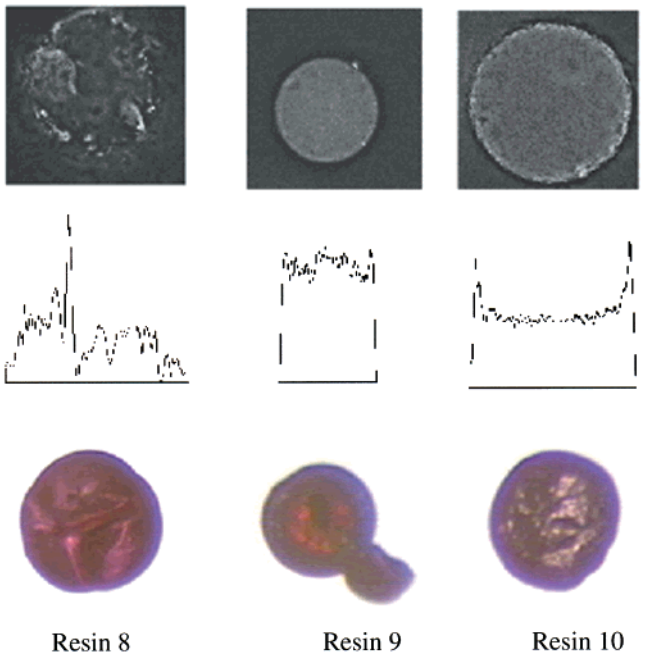

Figure 7. Other Rasta resins.

nonuniform clustering of dye with each cluster surrounded by unfunctionalized polystyrene (the dark areas within the bead). However, it is also observed that the polymerization process is not uniform (an important observation as this process is not unique to the synthesis of the Rasta resins), leading to several "centers" within a single bead. Resin **9**, much like **7**, shows fairly uniform distribution although only a single TMI molecule was initially incorporated at each TEMPO terminus in the LFRP step. Exposure of **1** to a 90 molar excess of polystyrene followed by a second round of LFRP with a mixture of styrene (35%) and TMI (65%) provides, after functionalization, resin **10**. In this instance, we anticipated to observe a resin akin to TentaGel or PS-*pf* wherein the dye would be confined predominantly to the outer edges of the resin bead as a clustered "shell" with an

unfunctionalized interior. Indeed, optical analysis data demonstrated this distribution of dye and indicated about 35−40% of the dye is located in the outer 5−10 μm. However, with the primary benzylic TEMPO functionality on **1**, a highly uniform growth of new polymer would not be expected.[6] Hence while there is a clear tendency for the dye to be localized toward the surface of **10**, some of the shorter chains will still localize dye in other regions of the bead. This distribution is also reflected by the nonfluorescent images captured and seen below the optical analysis data in Figure 7.

In conclusion, optical analysis experiments have demonstrated that Rasta resins such as **7** and **9** are uniformly functionalized throughout the entire bead. This suggests that reagents can diffuse completely throughout the bead during the LFRP functionalization and subsequent coupling process(es), providing a relatively uniform macromolecular environment fundamentally distinct from PS-*pf* and TentaGel for solid-phase synthesis and reagent scavenging. While the functional group distributions for Rasta resins are similar to that of ArgoPore and PS-*co*, the data collected clearly show that Rasta resins are more uniformly functionalized. In addition, Rasta resins feature much higher loading capacities and can be manipulated like standard polystyrene and TentaGel beads. The data collected for Rasta resins **8** and **10** further support that control may be exercised in the relative positioning of functional groups within Rasta beads by the addition of co-monomers as previously reported. The results presented here argue well for the use of Rasta resins for solid-phase synthesis and reagent scavenging.

Acknowledgment. The authors thank Mr. Jay Copeland and Professor Peter Sorger (MIT) for the generous use of their Deltavision unit for the collection of the optical analysis data and Professor Stuart Schreiber (Harvard, ICCB) for the use of his laboratory facilities. Professor Jie-Cheng Xu and colleagues from the Shanghai Institute of Organic Chemistry are graciously thanked for generous supplies of TEMPO resin and Joanne Rasmussen for helping with the graphics for this manuscript.

Supporting Information Available. General experimental procedures for a typical Rasta resin as well as additional optical analysis data. This material is available free of charge via the Internet at http://pubs.acs.org.

References and Notes

(1) (a) Hodges, J. C.; Harikrishnan, L. S.; Ault-Justus, S. Preparation of Designer Resins via Living Free Radical Polymerization of Functional Monomers on Solid Support. *J. Comb. Chem.* **2000**, *2*, 80−88. (b) Lindsley, C. W.; Hodges, J. C.; Filzen, G. F.; Watson, B. M.; Geyer, A. G. Rasta Silanes: New Silyl Resins with Novel Macromolecular Architecture via Living Free Radical Polymerization. *J. Comb. Chem.* **2000**, *2*, 550−559 and references therein.

(2) McAlpine, S. R.; Schreiber, S. L. Visualizing Functional Group Distribution in Solid-Support Beads by Using Optical Analysis. *Chem. Eur. J.* **1999**, *5*, 3528−3532.

(3) In all resins examined, similar data were obtained for multiple beads within each class.

(4) (a) Sarin, V. K.; Kent, S. B. H.; Merrifield, R. B. Properties of Swollen Polymer Networks. Solvation and Swelling of Peptide-Containing Resins in Solid-Phase Peptide Synthesis. *J. Am. Chem. Soc.* **1980**, *102*, 5463−5470. (b) Merrifield, R. B. The Role of the Support in Solid-Phase Peptide Synthesis. *Br. Polym. J.* **1984**, *16*, 173−178. (c) Vaino, A. R.; Goodin, D. B.; Janda, K. D. Investigating Resins for Solid-Phase Organic Synthesis: The Relationship Between Swelling and Microenvironment as Probed by EPR and Fluorescence Spectroscopy. *J. Comb. Chem.* **2000**, *2*, 330−336.

(5) Note: First, the cross section shown does not discuss the depth of the slice. The depth of the slice would dramatically alter the results of the autoradiography. Second, the resolution of autoradiography is typically lower than that for fluorescence, with the resolution ordinarily being much larger than 0.5 μm. It is not clear how the authors in ref 4a determined the resolution of their technique. This technique relies on the emission of photons, and these photons are captured in any direction from any position. Thus, the slice depth will vary the results dramatically, as will the saturation level of the photons, and therefore it is possible their observations are in fact consistent with our observations.

(6) Hawker, C. J.; Barclay, G. G.; Orellana, A.; Dao, J.; Devonport, W. Initiating Systems for Nitroxide-Mediated "Living" Free Radical Polymerization: Synthesis and Evaluation. *Macromolecules* **1996**, *29*, 5245−5254.

CC000068A